Zhou, W., Lowry, B., Wnuk, K., Liu, L., and Gutierrez, M. (2024) InSAR and Its Applications in Geo-Engineering: Case Studies with Different Platforms and Sensors, **In:** (M. Gutierrez Ed.) Information Technology in Geo-Engineering - Proceedings of 5th International Conference on Information Technology in Geo-Engineering, August 5 – 8, 2024, Golden, Colorado, USA, Publisher: Springer Nature Switzerland AG, 179 – 190.

InSAR and Its Applications in Geo-engineering: Case Studies with Different Platforms and Sensors

Wendy Zhou[1[0000-0001-8226-375X]] Benjamin Lowry[2[0000-0001-6357-6363]] Kendall Wnuk[3[0000-0001-7499-5256]] Linan Liu[4[0000-0003-2944-0889]] and Marte Gutierrez[5[0000-0001-5070-8926]]

[1] Colorado School of Mines, Golden, CO 80401, USA wzhou@mines.edu
[2] Solid Ground Geospatial, Golden, CO 80401, USA
ben.lowry@solidgroundgeo.com
[3] Colorado School of Mines, Golden, CO 80401, USA kwnuk@usgs.gov
[4] China University of Geosciences (Beijing), Beijing, China, 100190
linanliu@cugb.edu.cn
[5] Colorado School of Mines, Golden, CO 80401, USA
mgutierr@mines.edu

Abstract. InSAR (Interferometric Synthetic Aperture Radar) is a microwave remote sensing technique that uses the phase shift of radar signals acquired at different timeframes to measure or monitor ground deformation. InSAR has many implications, such as monitoring ground deformation caused by natural- or geo-hazards, e.g., earthquakes, volcanoes, landslides, anthropogenic activities, groundwater pumping, underground mining, and hydrocarbon extraction. InSAR can also be utilized to study infrastructure displacements and environmental changes, such as monitoring changes in surface water level, mapping floods, soil moisture contents (at a shallow depth), and deforestation. The first significant application of SAR is the deployment of real-aperture radar interferometry to study the topography of the Moon in the early 1970s. However, InSAR was not widely used due to the limitations of computation capacity and the sparse available SAR data until the early 1990s. A major milestone for InSAR applications came in the 1990s when researchers used SAR data to measure ground deformation induced by the Landers Earthquake in California, and one of the publications landed on the cover of Nature magazine. This landmark achievement brought widespread recognition to the potential of InSAR for mapping ground deformation. Over the past two decades, the computation power and availability of SAR data have improved considerably with the launch of more satellites carrying SAR sensors. This paper presents a brief introduction to the history and fundamentals of InSAR, as well as case studies of its applications in the geo-engineering fields, including landslide displacement monitoring and underground excavation-induced ground subsidence mapping.

Keywords: InSAR, Landslide Displacement Mapping, Tunnelling-induced Ground Subsidence Monitoring.

1 Introduction

The theoretical basis for Radio detection and ranging (RADAR) technology in the context of electricity and magnetism has existed since the late 19th century (Maxwell, 1873). Radar systems use the microwave portion of the electromagnetic spectrum at wavelengths from 1 millimeter (corresponding frequency 300 GHz) to 1 meter (corresponding frequency 300 GHz) (Vollmer, 2004).

Early experiments using InSAR techniques were conducted in the 1970s. Zisk (1972) used ground-based side-looking real-aperture radar Interferometry to study the topography of an area on the Moon, including the craters Ptolemaeus, Alphonsus, and Arzachel and a portion of Mare Nubiumn. Rumsey et al. (1974) used the brightness and altitude of Radar images to study the craters' geometry and topography on a portion of Venus. In the late 1980s, Gabriel et al. (1989) used three Seasat (the first Earth-orbiting satellite designed for remote sensing of the Earth's oceans) observations to study the swelling of water-absorbing clays of an area in the Imperial Valley, California.

However, InSAR did not become widely used until the early 1990s due to computers' insufficient calculation capacity and the lack of an abundant amount of SAR observation data available. In 1991, the launch of the European Remote Sensing Satellite (ESR-1) brought more SAR observation data. ESR-1 was the first Earth-observing Satellite by the European Space Agency (ESA). Among all instruments, it carried a SAR sensor operating in the C band, with a wavelength of 5.7 cm (corresponding frequency of 5.3 GHz). A major milestone for InSAR applications arrived in the 1990s when researchers used SAR data from the ERS-1 to measure ground deformation induced by the Landers earthquake in California (Massonnet et al., 1993; Zebker et al., 1994). These publications brought wide attention to the potential of InSAR applications. In 1995, ESR-2 was launched. Publications related to elevation measurement and ground deformation using InSAR reverberated in both quantity and quality.

Over the past decades, the computation power and availability of SAR data have improved dramatically with the launch of more satellites with SAR sensors (Table 1). InSAR has become a commonly used powerful ground deformation monitoring technique for an array of applications (e.g., Shen and Ye, 1998; Dzurisin and Lu, 2006; Lu and Dzurisin, 2014; Milillo et al., 2018; Werner et al., 2016; Wnuk et al., 2019; Zhou et al., 2006; Bürgmann et al., 2000).

Table 1. A Summary of Synthetic Radar Satellites Missions and Sensors

Satellite Missions	Duration	Band	Revisit Time (days)
European ERS-1	1991-2000	C-band	35
Japanese JERS-1	1992-1998	L-band	44
European ERS-2	1995-2021	C-band	35
Canadian Radarsat-1	1995-	C-band	24
European Envisat	2002-2010, 2010-2012	C-band	35, 30
Japanese ALOS-1	2006-2011	L-band	46

German TerraSAR-X / TanDEM-X	2007-	X-band	11
Italian COSMO-SkyMed	2007-	X-band	16
Canadian Radarsat-2	2007-	C-band	24
German TanDEM-X	2010-	X-band	11
Korean KOMPSAT-5	2013-	X-band	28
Japanese ALOS-2	2014-	L-band	14
European Sentinel-1A	2014-	C-band	12
Spanish PAZ	2018-	X-band	11
Argentinian SAOCOM-1	2018-	X-band	16
Italian COSMO-SkyMed Second Generation	2019-	X-band	16
Canadian Radarsat Constellation	2019-	C-band	12
Korean KOMPSAT-6	2023-	X-band	28

X-band: wavelength = ~3 cm; C-band: wavelength = ~5.7 cm; L-band: wavelength = ~24 cm

2 InSAR Basics

Imaging radar is an active remote sensing system, i.e., satellites transmit microwaves and receive the return signal. Synthetic aperture radar (SAR) is an advanced radar system that utilizes image processing techniques to "synthesize" a large antenna to achieve much higher spatial resolution than a traditional radar. Every pixel in a SAR image carries two pieces of information – the amplitude and the phase. SAR backscattering amplitude is sensitive to terrain slope, surface roughness, and dielectric constant. The SAR backscattering phase is related to the distance from the satellite to the ground. The long wavelength of microwave radiation can penetrate through cloud cover, haze, dust, rain, and darkness, which allows the detection of microwave energy under almost all weather and environmental conditions.

The radar beam is transmitted at a slant direction at right angles to the direction of flight. It illuminates a **swath** while the satellite or aircraft is flying forward. The **range** is the across-track dimension perpendicular to the flight direction. **Azimuth direction** refers to the along-track dimension parallel to the flight direction. **The incidence angle** is the angle between the vertical direction and the radar beam. The **slant range distance** is the radial line of sight (LoS) distance between the radar and each target on the surface. The **ground range** distance for any point with the swath is the true horizontal distance from the nadir point. A radar's spatial resolution depends on the properties of microwave radiation and geometrical effects. The **range, or across-track resolution,** depends on the length of the pulse (P). The **along-track resolution** is determined by the angular width of the radiated radar beam and the slant range distance (Fig. 1).

There are different modes of radar beam scanning, such as strip map mode and spotlight. Spotlight mode can produce higher spatial resolution images. In addition, the SAR sensor can be mounted on different platforms, such as terrestrial, airborne, and spaceborne.

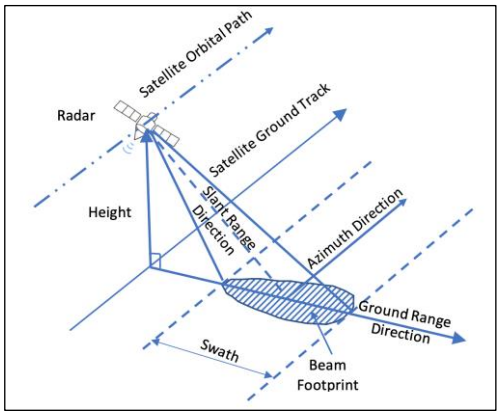

Fig. 1. A schematic of the side-looking viewing geometry and spatial resolution.

If two radar images are acquired at different times from the same place, differential movement will result in a different measured phase. An "interferogram" is a complex image. Its magnitude is related to the correlation of the images, and phase is related to geometry difference. InSAR Differential interferometric phase is a sum of several components (Equation 1).

$$\Delta\phi = \phi_{topographic} + \phi_{deformation} + \phi_{atmospheric} + \phi_{orbit} + \sigma_{noise} \quad (1)$$

where $\phi_{topography}$ is the phase change due to topographic variation, $\phi_{deformation}$ is the phase change caused by ground deformation, $\phi_{atmospheric}$ is the phase change due to atmospheric noise, ϕ_{orbit} is the phase change due to orbital error, and σ_{noise} is the phase change due to instrument noise.

The LoS displacement over time is calculated by equation (2).

$$\delta_{line\text{-}of\text{-}sight} = -\lambda\Delta\phi / 4\pi \quad (2)$$

where $\delta_{line\text{-}of\text{-}sight}$ is the LoS displacement over the time of two radar image acquisitions, λ is the radar wavelength, and $\Delta\phi$ is the phase shift of backscatter signals calculated by equation (1).

In cases of poor signal-to-noise ratios, advanced InSAR proposing methods, such as multi-temporal InSAR, small baseline subset InSAR, persistent scatterer InSAR, and interferometric point target analysis, need to be used to overcome the limitations of pf InSAR in monitoring ground subsidence. Through the use of advanced InSAR techniques, one can remove error sources based on their spatial and temporal characteristics, improve the accuracy of ground deformation measurement, and provide time-series deformation measurements.

3 Case Studies of InSAR Applications in Geo-Engineering

This section is a synthesis of a series of research projects conducted at the Colorado School of Mines. InSAR technology has been applied to mapping ground displacement due to landslides, and underground excavations through a few case studies: (i) a

slow-moving landslide monitoring using ground-based radar interferometry in Granby, Grand County, Colorado, USA, (ii) new landslide activity recognition using ALOS-1 InSAR in Gunnison County, Colorado, USA, (iii) mapping 3D deformation induced by urban excavation using multiplatform InSAR time-series analysis in Los Angeles, California, USA and (iv) twin-tunneling-induced uneven ground subsidence mapping using Sentinel-1 InSAR and parametric study using machine learning in downtown Los Angeles, California, USA.

Colorado experiences many landslides each year because of its steep terrain, from west of the Front Range to the Western Slope. Some of these areas are difficult to access. On the other hand, ground subsidence is of great concern in urban settings, especially when conducting projects dealing with soft ground and shallow excavations. The above-ground structures and facilities must not be impacted beyond a certain deformation threshold. The first two case studies presented next focus on mapping the deformation rate of landslides in Colorado using the Interferometry of ground-based SLAR and Satellite-based SAR. The last two case studies focus on ground subsidence induced by underground excavations in urban environments.

3.1 A Slow-Moving Landslide Monitoring Using Ground-Based Radar Interferometry in Granby, Grand County, Colorado, USA

The Granby landslide has a surface area of ~160,000 m^2 (40 acres) and is moving in a southwesterly direction. In ground-based platforms, the radar scanning location can be positioned to reduce the effects of the obliquity between the radar's LoS and the direction of landslide displacement.

The ground-based **G**amma **P**ortable **R**adar **I**nterferometer (GBIR) was deployed to monitor the slow-moving, translational failure landslide in Granby, Grand County, Colorado, USA. GBIR scanning was completed over two separate surveys in the summer of 2011. The purpose of this work is to evaluate GBIR as a temporally dense monitoring technique for monitoring landslide displacement and compare the monitoring results to the then ongoing GPS-based surveying methods to verify measured displacements. Since the GBIR system is a rotational scanner, the LoS obliquity varies azimuthally across the scene. A final displacement was transformed from LoS to horizontal displacement, using an average movement direction from previous surveys of monument displacements (Fig. 2).

The GBIR-measured displacements were compared with the GPS survey measurements**.** The GPS surveying was conducted independently as part of ongoing stabilization activities. Comparisons with GPS were conducted by selecting the pixel on an unwrapped interferogram where the monument was located. Landslide displacement using the GPRI sensor is capable of detecting and monitoring displacement. The real-aperture rotational radar sensor requires a customized approach for landslide monitoring. Images generated from radar scanning were of sufficient quality to generate interferograms that could be used to derive displacements in mm-scale and useful in resolving small-scale temporal variation in slip rates. The measurements of GBIR scanning and traditional GPS surveys were compared, and the results were agreed well (Fig. 3). The GBIR scanning has the advantage of providing continuous distribution of displacement rate over the study area, while GPS surveys only provide point measurements.

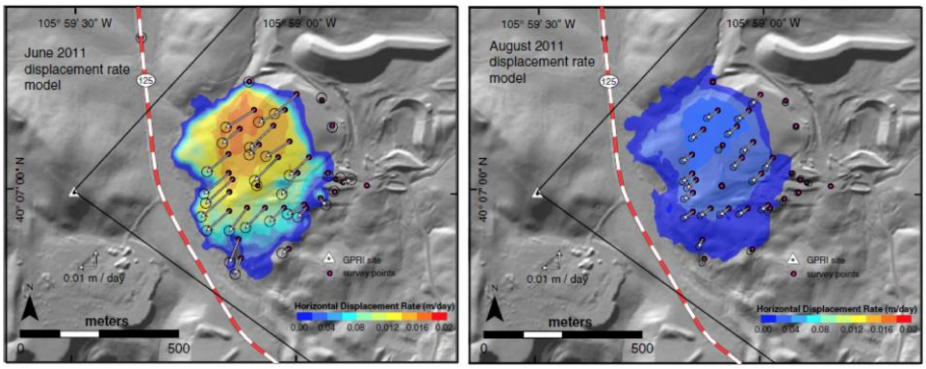

Fig. 2. Radar-derived daily horizontal displacement rate (modified from Lowry et al., 2013)

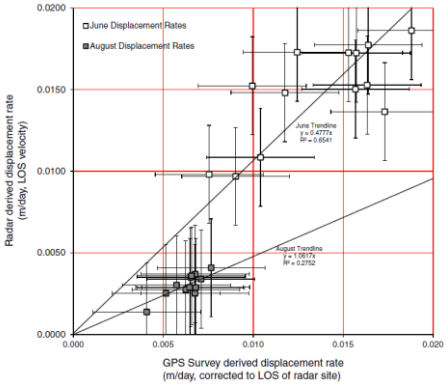

Fig. 3. The comparison shows general agreement and clearly indicates the higher displacement rate of the landslide in June and the lower displacement rate in August (Lowry et al., 2013).

3.2 New Landslide Activity Recognition Using ALOS-1 InSAR in Gunnison County, Colorado, USA

The East Muddy Creek Landslide Complex (EMCLC) in Colorado, USA, consists of three individual landslides. The EMCLC experienced multiple activation and deactivation periods over several decades. The reactivation in the 1980s destroyed Colorado State Highway 133 and blocked the highway from 1986 to 1987. The EMCLC has been investigated by state and federal agencies, but the landslide boundary delineated by these investigations was constrained by the locations where the in-situ instruments were installed.

This case study used Advanced Land Observing Satellite-1 (ALOS-1) InSAR analysis and recognized new landslide activity by comparing the result from ALOS-1 InSAR to traditional field methods for ground motions at a watershed scale. Previous studies suggested that the EMCLC is within a much smaller area (Fig. 4). This effort recognized a larger zone of landslide creep with ALOS-1 InSAR.

Line of Sight (LoS) velocity mapping is used to characterize displacement zonation, failure modes, and hazard assessment activities. The landslide dynamics were

deliberated based on the InSAR results and existing geological modeling. ALOS-1 InSAR analysis reveals newly detected ground displacement at very slow to extremely slow rates with a significantly increased spatial extent. Patterns of deformation rate profiles and comparison with morpho-structures indicate that the translational regime of landslide motion is validated, with some evidence of complex movement in the upper reaches of the 2500 m distance from the valley bottom (Fig. 5).

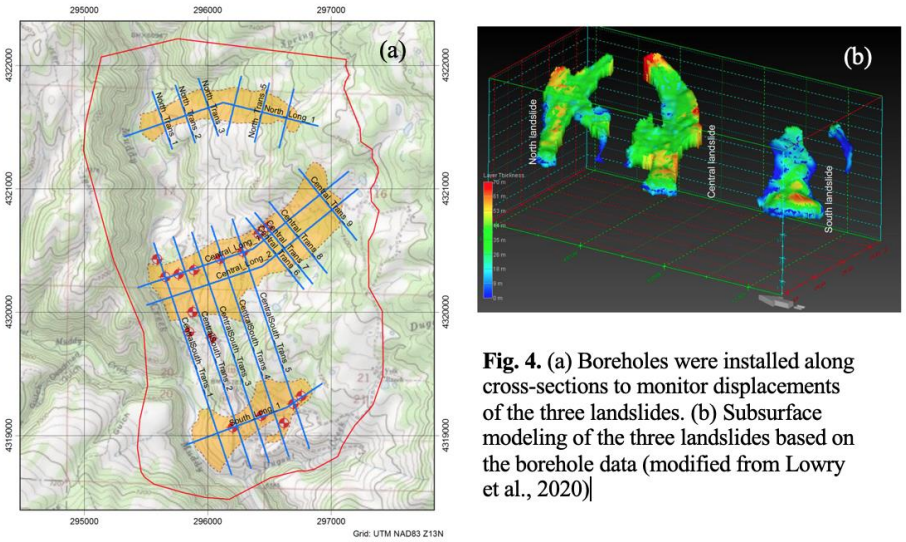

Fig. 4. (a) Boreholes were installed along cross-sections to monitor displacements of the three landslides. (b) Subsurface modeling of the three landslides based on the borehole data (modified from Lowry et al., 2020)

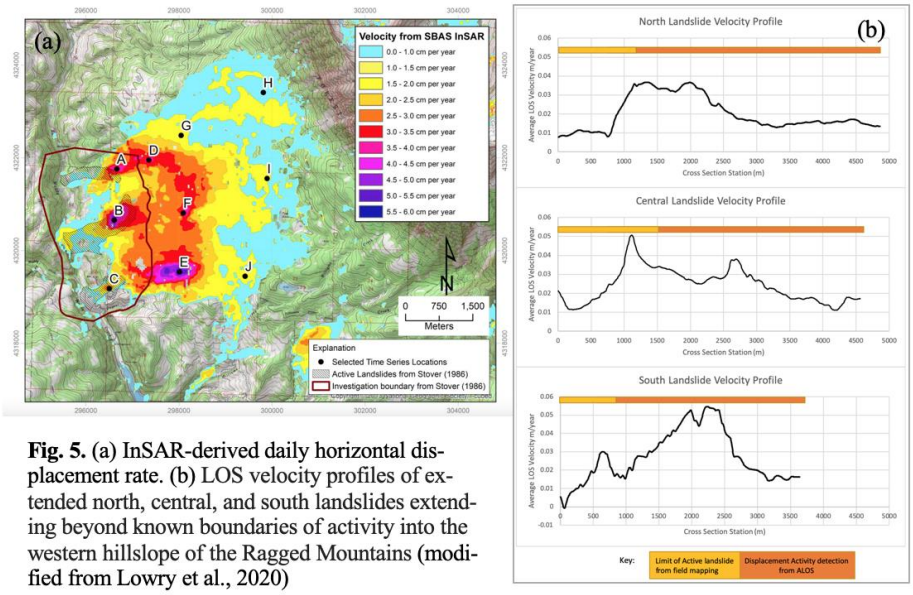

Fig. 5. (a) InSAR-derived daily horizontal displacement rate. (b) LOS velocity profiles of extended north, central, and south landslides extending beyond known boundaries of activity into the western hillslope of the Ragged Mountains (modified from Lowry et al., 2020)

3.3 Measuring 3D Deformation Induced by Urban Excavation Using Multiplatform InSAR Time-Series in Los Angeles, California, USA

Excavation of a subway station and rail crossover cavern in downtown Los Angeles, California, USA, induced over 1.8 cm of surface settlement between June 2018 and February 2019 as measured by a ground-based monitoring system. In this study, point measurements of surface deformation above the excavation were extracted by applying InSAR time-series analyses to datasets from multiple sensors with different wavelengths. These sensors include C-band Sentinel-1, X-band COSMO-SkyMed, and L-band Uninhabited Aerial Vehicle SAR (UAVSAR) (Fig. 6). The airborne SAR data with alternative viewing geometries to traditional polar-orbiting SAR satellites were used to constrain horizontal displacements in the North-South direction while maintaining agreement with ground-based data.

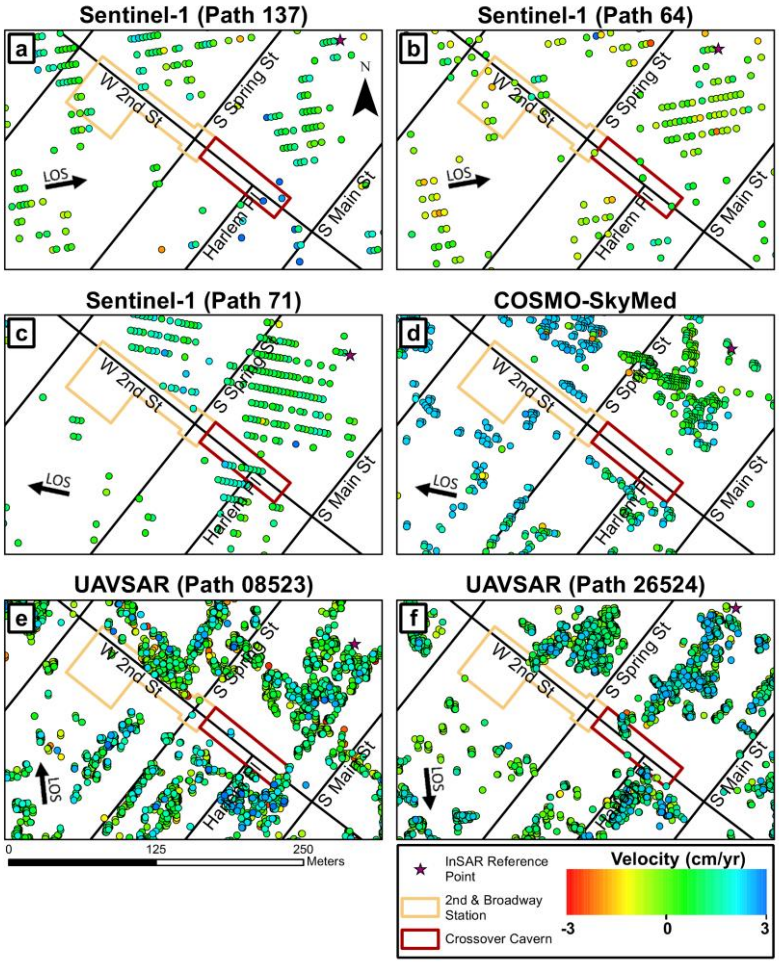

Fig. 6. (**a**–**f**) Persistent scatterer locations and LoS velocity directions associated with spaceborne and airborne InSAR datasets (Wnuk et al., 2021).

The InSAR time-series point measurements, produced from integrated satellite and airborne SAR datasets from X, C, and L band sensors, were interpolated to continuous distribution surfaces, weighted by distance, and entered into the Minimum-Acceleration (MinA) algorithm to calculate 3D displacement values (Pepe et al., 2016). The results from this study revealed previously unidentified deformation surrounding the 2nd Street and Broadway Subway Station and the adjacent rail crossover cavern, with maximum vertical and horizontal deformations reaching 2.5 cm and 1.7 cm, respectively.

Excavation of the crossover cavern took place between May 30, 2018, and March 14, 2019. It is only ~15m below the surface in weathered sedimentary rock. During this excavation, the Network of Ground Surface Settlement Points (GSSP) measured nearly 2cm of subsidence along the overlying infrastructure. Vertical displacements calculated by combining six paths of InSAR data were in good agreement. However, the discrepancy with available ground-based data is within 5 mm on average.

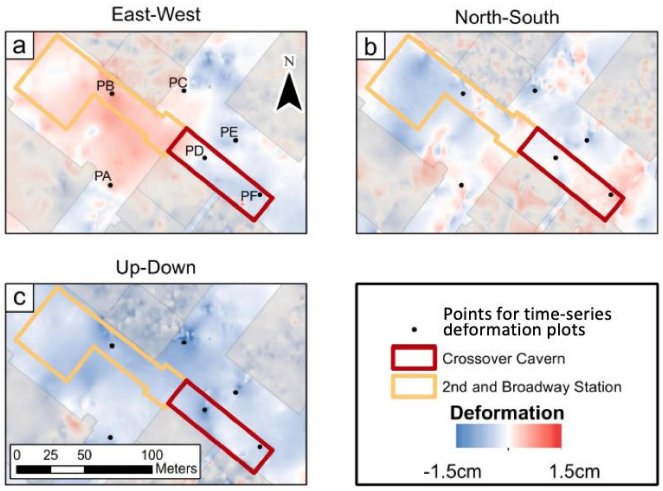

Fig. 7. Map of surface deformation calculated from InSAR data spanning 16 November 2018 to 21 February 2019 in (**a**) East-West, (**b**) North-South, and (**c**) Up-Down directions (modified from Wnuk et al., 2021).

3.4 Twin-Tunneling-Induced Uneven Ground Subsidence Mapping Using Sentinel-1 SAR Interferometry and Parametric Study Using Machine Learning in Downtown Los Angeles, USA

The Regional Connector Transit Corridor (RCTC) project in downtown Los Angeles constructs 3.1 km long twin-bore tunnels, crossover caverns, and three stations between tunnel sections. Case study 3 examined the ground deformation due to the excavation of the crossover cavern and the 2nd and Broadway Station. Most sections of the Regional Connector tunnels were excavated using a pressurized-face Tunnel Boring Machine (TBM) with an excavated diameter of approximately 6.7 meters, though some sections used the cut-and-cover construction method. The two tunnels were completed by late 2017 and January 2018, respectively.

This case study focuses on the ground subsidence induced by the excavation of the twin tunnels. These tunnels traverse complicated ground conditions of cohesive alluvium soils and soft rock beneath the heavily populated urban environment. PSInSAR was utilized to measure ground subsidence induced by the twin-tunnel excavation using both descending and ascending Sentneil-1 datasets. Permanent Scatterers (pixels display both stable amplitude and a coherent phase over time) were identified in order to mitigate relatively higher noises in urban environments.

Twin-tunneling-induced ground settlement is dominantly vertical. In this study, the vertical deformation rate is derived by combining Line of Sight (LoS) deformation velocities obtained from SAR images from both ascending and descending satellite orbits. Our study revealed local and uneven subsidence up to approximately 12 mm/year along the tunnel alignment (Fig. 8). In order to identify factors associated with the uneven subsidence, a Machine Learning (ML)-based permutation feature importance method is used for a parametric study. Groundwater level, overburden thickness, the distance between the two tunnel centerlines, the depth of the tunnel springline, above-ground building height, and the distance between the building and the tunnel centerlines were used for the parametric study. The analysis shows that overburden thickness is the most dominant factor. In addition, the uneven settlements are geologically sensitive and more concentrated in areas with thick artificial fill and alluvium soils.

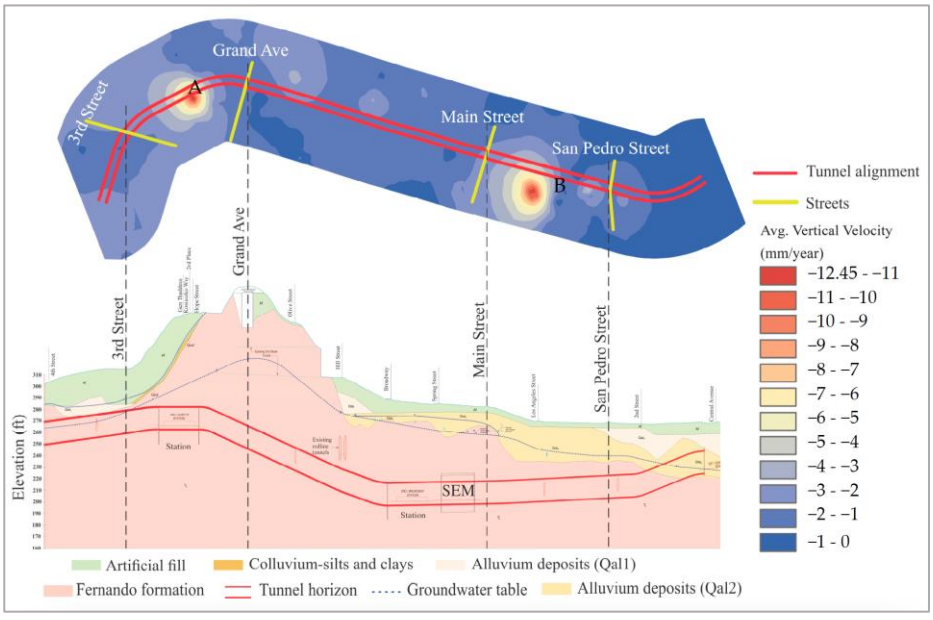

Fig. 8 Ground settlement field and corresponding geological conditions (Liu et al., 2023)

4 Summary

The history and fundamentals of InSAR are briefly introduced in this paper. In addition, the applications of InSAR in the context of geo-engineering were demonstrated through four case studies. The capacities of InSAR can elevate the analyses and bring new findings that were nearly impossible to discover by the traditional survey methods. The advanced InSAR analyses presented in this paper include (1) mapping millimeter-level landslide daily displacement rate using GAMMA ground-based interferometric radar (GBIR), (2) recognizing new landslide activity and deformation patterns using ALOS-1 InSAR analysis, (3) mapping 3D deformation induced by urban excavation using multi-sensors and platforms SAR datasets, including C-band Sentinel-1, X-band COSMO-SkyMed, and L-band Uninhabited Aerial Vehicle SAR (UAVSAR), and (4) mapping twin-tunneling-induced uneven ground settlement using Sentinel-1 PSInSAR and identify factor(s) associated with the uneven subsidence using a parametric study via a Machine Learning (ML)-based permutation feature importance method.

Traditional survey methods for ground displacement are essential for the verification of InSAR results. Traditional field measurements and InSAR analysis are complementary, and the combination of these two is essential for advancing knowledge of ground displacement dynamics. Traditional methods collect first-hand data, and InSAR brings the analysis to a new depth in a time-effective and cost-efficient fashion.

Last but not least, there are limitations to the InSAR technique. These limitations include but are not limited to (1) one-dimensional measurement at the line of sight (LoS) direction, (2) atmospheric noise is difficult to model and remove, (3) heavily vegetated areas, areas with steep terrains, and areas too small are challenging to produced meaningful InSAR results, (4) InSAR does not work well if deformation rate is too large, (5) temporal decorrelations of SAR observations need to be handled, (6) the near-polar satellite orbits of SAR is not sensitive to north-south orientated ground deformation, and (7) InSAR results are often algorithm, software or operator dependent. However, one should not be discouraged by these limitations. As demonstrated by the four case studies, high-quality InSAR analysis results can be achieved by carefully navigating these limitations.

References

1. Bürgmann, R., Rosen, P.A. Fielding, E. J.: Synthetic Aperture Radar Interferometry to Measure Earth's Surface Topography and Its Deformation. Annual Review of Earth and Planetary Sciences 28, 169-209 (2000).
2. Dzurisin, D., Lu, Z.: Interferometric synthetic-aperture radar (InSAR). In: Dzurisin, D (Ed.), Volcano Deformation: New Geodetic Monitoring Techniques, pp. 153-193. Springer Science & Business Media (2006).
3. Gabriel, A.K., Goldstein, R.M., and Zebker, H.A.: Mapping small elevation changes over large areas: Differential radar interferometry. Journal of Geophysical Research 94, 9183-9191 (1989).

4. Lowry, B., Gomez, F., Zhou, W., Mooney, M.A., Held, B., Grasmick, J.: High Resolution Displacement Monitoring of a Slow Velocity Landslide using Ground Based Radar Interferometry. Engineering Geology 166 (8), 160-169 (2013).
5. Lowry, B. W., Baker, S., Zhou, W.: A Case Study of Novel Landslide Activity Recognition Using ALOS-1 InSAR within the Ragged Mountain Western Hillslope in Gunnison County, Colorado, USA. Remote Sensing 12(12), 1969 (2020).
6. Lu, Z., Dzurisin, D.: InSAR Imaging of Aleutian Volcanoes Monitoring a Volcanic Arc from Space. P. 390, Springer, Berlin, Heidelberg. (2014).
7. Liu, L., Zhou, W. Gutierrez, M.: Mapping tunneling-induced uneven ground subsidence using Sentinel-1 SAR Interferometry: A twin-tunnel case study of downtown Los Angeles, USA. Remote Sensing 15 (1), 202 (2023).
8. Maxwell, J.C.: A Treatise on Electricity and Magnetism. Nature 7, 478-480 (1873).
9. Massonnet, D., Rossi, M., Carmona, C. *et al.* The displacement field of the Landers earthquake mapped by radar interferometry. Nature 364, 138–142 (1993).
10. Milillo, P., Giardina, G., DeJong, M.J., Perissin, D., Milillo, G.: Multi-temporal InSAR structural damage assessment: The London Crossrail case study. Remote Sensing 10, 287 (2018)
11. Pepe, A., Solaro G., Calò, F., Dema, C.: A Minimum Acceleration Approach for the Retrieval of Multiplatform InSAR Deformation Time Series. IEEE Journal of Selected Topics in Applied Earth Observations and Remote Sensing 9, 3883–3898 (2016).
12. Rumsey, H. C., Morris, G. A., Green, R. R., Goldstein, R. M.: A radar brightness and altitude image of a portion of Venus. Icarus 23(1), 1-7 (1974).
13. Vollmer, M.: Physics of the microwave oven. Physics Education 39(1), 74 (2004). https://doi.org/10.1088/0031-9120/39/1/006
14. Shan, XJ., Ye, H.: The INSAR technique: its principle and applications to mapping the deformation field of earthquakes. Acta Seismologica Sinca 11, 759–769 (1998).
15. Werner, C.; Lowry, B.; Wegmuller, U.; Pugh, N.; Schrock, G.; Zhou, W. Deformation time-series derived from terrestrial radar observations using persistent scatterer interferometry in Seattle, Washington. In Proceedings of the 2016 IEEE International Geoscience and Remote Sensing Symposium (IGARSS), Beijing, China, 10–15 July 2016; pp. 6835–6838.
16. Wnuk, K.; Walton, G.; Zhou, W. Four-dimensional filtering of InSAR persistent scatterers elucidates subsidence induced by tunnel excavation in the Sri Lankan highlands. Journal of Applied Remote Sensing 13, 034508 (2019).
17. Wnuk, K., Zhou W. Gutierrez, M.: Mapping Urban Excavation Induced Deformation in 3D via Multiplatform InSAR Time-Series. Remote Sensing 13(23), 4748 (2021).
18. Zebker, H. A., Rosen, P. A., Goldstein, R. M., Gabriel, A., Werner, C. L.: On the derivation of coseismic displacement fields using differential radar interferometry: The Landers earthquake. Journal of Geophysical Research 99, 19617–19643 (1994).
19. Zhou, W., Chen, G., Li, S., Ke, J.: InSAR Application in Detection of Oilfield Subsidence on Alaska North Slope. In Proceedings of the 41st US Symposium on Rock Mechanics (USRMS), ARMA-06-986, pp.1-11, OnePetro, Golden, Colorado, USA, (2006).
20. Zisk, S. H.: Lunar Topography: First Radar-Interferometer Measurements of the Alphonsus-Ptolemaeus-Arzachel Region. Science 178(4064), 977-980 (1972).